Analysis of the geometry of the growth ridges and correlation to the thermal gradient during growth of silicon crystals by the Czochralski-method

L. Stockmeier[1,2], C. Kranert[1,2], P. Fischer[1,2], B. Epelbaum[1], C. Reimann[1,2], J. Friedrich[1,2], G. Raming[3], A. Miller[3]

[1] *Fraunhofer IISB, Schottkystraße 10, 91058 Erlangen, Germany*

[2] *Fraunhofer THM, Am St.-Niclas-Schacht 13, 09599 Freiberg, Germany*

[3] *Siltronic AG, Johannes-Hess-Straße 24, 84489 Burghausen, Germany*

Abstract

A contactless, non-destructive approach to measure the geometrical parameters of the growth ridge, based on surface topography, is presented and established. It allows a systematic, large scale analysis of growth ridges of single crystals of almost any type. Here, it is applied to Czochralski-grown silicon crystals. Based on the measurement results, Voronkov's theory of the shape of the growth ridge is verified. This theory is used to calculate the temperature gradient at the growth ridge from the geometrical parameters. The presented method gives an easy, direct experimental access to the thermal conditions, both qualitative and quantitative, at the solid-liquid interface during the growth process.

1. Introduction

In the Czochralski (Cz) as well as in the Floating Zone (Fz) technique the crystal typically grows in a cylindrical shape due to crystal rotation which averages out thermal

asymmetries. However, from a cross sectional viewpoint minor deviations from a perfectly circular disk always exist. These deviations can be seen as ridge-like protrusions and are caused by the local growth of atomically smooth facets, leading to the formation of so-called growth ridges or growth lines (see Fig. 1). They have been observed for a variety of crystal materials like semiconductors (Si, Ge) as well as oxides ($LiNBO_3$, garnet).

In general the occurrence of growth ridges and related edge facets is a result of the differing growth kinetics of atomically rough and smooth interfaces. For example, in cylindrical <100>-oriented dislocation-free Cz or Fz Si crystals, four {111} edge facets appear along the <110> directions perpendicular to the growth axis. The atomically rough interface already grows already at a very small supercooling ΔT below 0.001 K [1, 2], whereas the growth ridges are formed at the crystal periphery near the three phase line (TPL) by the formation of a two-dimensional nucleus on the atomically smooth {111} facets requiring a relatively large supercooling ΔT of 3.7 K [3]. Then the 2D nucleus grows with a high velocity laterally along the {111} plane. As a result, the internal {111} plane lags behind the rest of the growing rough interface.

The presence of the {111} edge facet also influences the height of TPL, the free surface orientation and the growth angle, causing the TPL to rise at the {111} facet and the crystal to grow outwards in this region. This rise of the TPL is accompanied by a change of the shape of the melt meniscus which then bends inwards, stopping the outward growth. This growth mechanism leads to these ridge-like protrusions at the external surface of the crystal [4].

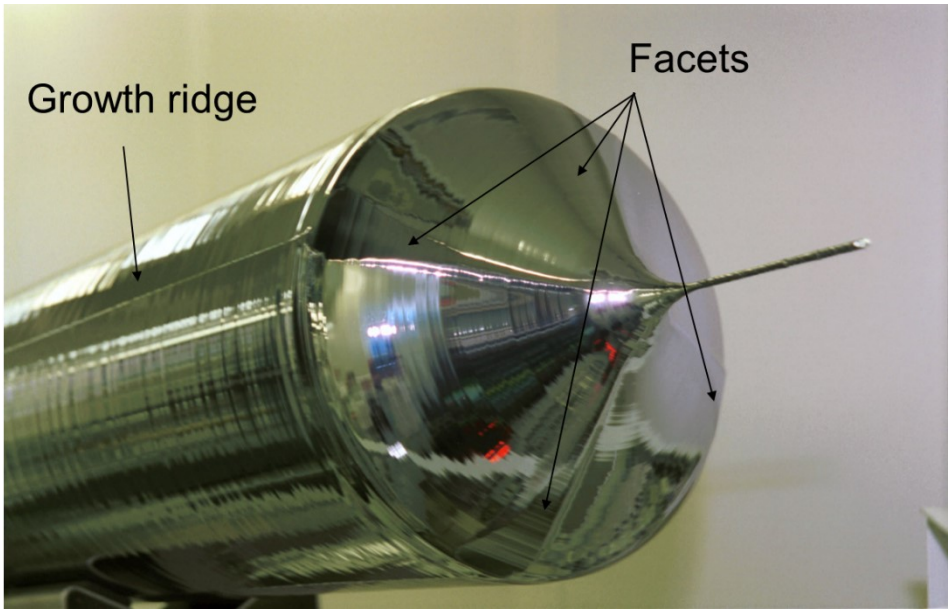

Fig. 1 <100>-oriented Cz-grown Si crystal with a diameter of 300 mm. On the shoulder, four {111} facets are visible along the four <110> directions. On the cylindrical surface, the facets shrink to the so-called growth ridges.

Four different cases regarding the geometry of growth ridges can be distinguished, as depicted in Fig. 2:

1. If the growth ridge is formed solely due to the formation of internal edge facets within the crystal, as described in the introduction, a bump is formed.
2. If the outer crystal surface coincides with a {111} plane, an external facet may form on top of this bump, which has a mirror like appearance and is called mirror facet.
3. If the crystal surface oscillates (for instance because of periodic instability of the meniscus) closely around the plane of the external facet, so-called pseudo facets may form [4]. In this case the formation of the external facet is disrupted frequently, leading to steps on the crystal surface [5].

4. In the course of crystal diameter decrease (the case of the end cone), the edge facet can become the external facet. The growth of an internal facet does not occur due to a lack of supercooling in the respective direction.

The present publication focusses on growth ridges of type 1 formed due to internal edge facets along the crystal body of constant diameter. The other cases, where external facets may occur, are not discussed here.

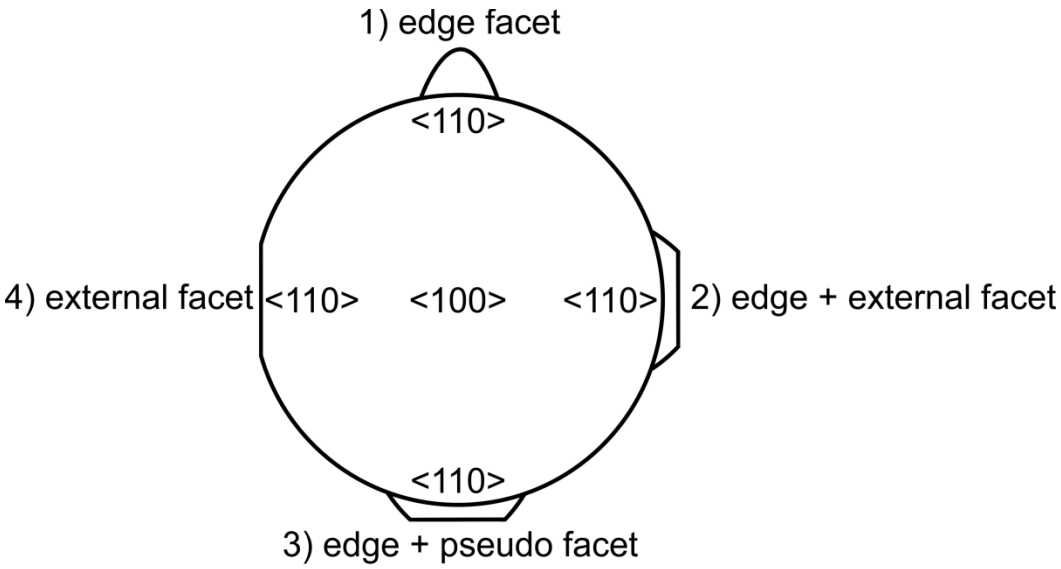

Fig. 2 Overview of different types of growth ridges which can occur during the growth of a <100> oriented Si crystal.

The presence of the growth ridges during growth of Cz and Fz silicon crystals is commonly used as an indicator whether the crystal is growing dislocation-free [6, 7]. When dislocations form during the growth process, the growth kinetics of the facet planes change [8], leading to a reduction of the necessary supercooling for the edge facets to grow. Thus, the length of the edge facets will be affected and as a result the growth ridge will alter its shape or even vanish.

Voronkov [3, 9, 10] was the first to develop a detailed theoretical understanding for the growth phenomena at the edge facets and the related growth ridges. Later on, Barinovs [11] obtained a simple analytical expression for the geometry of the growth ridge from Voronkovs' theoretical model and implemented it in a numerical algorithm to calculate the size of the growth ridge from known temperature gradients. These theoretical works predict a strong correlation between growth ridge geometry and thermal field. That means that the growth ridge carries quantitative information about the thermal field during the growth process. So far, such information can only be obtained by direct temperature measurements in dedicated experimental runs or by numerical simulations [12]. An accurate geometrical analysis of the growth ridge can provide a simple, non-destructive access to such information, highly desirable as fast feedback for the crystal grower. However, an extensive experimental analysis of the growth ridge shape has not been performed yet.

We propose a method to determine the geometry of growth ridges on the surface of Si crystals by contactless surface measurements. For verification, these optical measurements of the crystal surface are compared to a microscopic analysis of the edge facets using defect-selectively etched samples and to theoretical predictions. Finally, we present an exemplary comparison of two crystals from different growth processes, illustrating the potential of this method.

2. Theory

The key parameter describing the formation of a growth ridge is the deviation of the meniscus angle from the undisturbed case of non-faceted growth, $\delta\phi_c$. Stable growth

requires a compensation for that disturbance. According to Voronkov [10], in case of edge facets only (case 1 in Fig. 2), the compensating parameter $\delta\phi_{\mathrm{m}}$ takes the form

$$\delta\phi_{\mathrm{m}} = -\chi + \frac{2}{a}\frac{\Delta T}{G} \tag{1}$$

where χ is the deviation between apparent and intrinsic growth angle[10], a is the capillary constant ($a = 0.76\,\mathrm{cm}$ for large diameter Cz silicon [13]) and ΔT is the supercooling required for {111} facet growth in silicon. Voronkov states that G is supposed to be the axial temperature gradient, but the relevant parameter for facet growth is the component of the temperature gradient along the facet plane, g_{facet}. In the following, we therefore use g_{facet} instead. Voronkov [10] further found a relation between the value $\delta\phi_{\mathrm{m}}$, the growth ridge width w and the growth ridge depth d:

$$\delta\phi_{\mathrm{m}} = -\frac{4\mathrm{d}}{w} \tag{2}$$

Using the fact that the facet depth d is simply the projection of the facet length l (along the [112] direction) from the (111) plane into the (100) plane (along the [110] direction), i.e. $d = l\sin\psi_{111}$, and that $l = \frac{\Delta T}{g_{\mathrm{facet}}}$, the combination of eqs. 1 and 2 yields that d and w are connected by constant values only:

$$d = \frac{\chi}{2\left(\frac{2}{w} + \frac{1}{a\sin\psi_{111}}\right)} \tag{3}$$

Here, ψ_{111} is the angle between the {111} facet plane and the pulling direction, which is $\psi_{111} = 54.74°$ for growth in the [001] direction.

As confirmed below by the experimental results, the growth ridge can be approximately assumed to be triangularly shaped. Within this approximation, the surface of the growth

ridge for a single facet can be described as two vectors in the (111) plane. The angle between these vectors is determined by the value ratio between growth ridge width w and depth d (see eq. 2), which in turn solely depends on the temperature gradient (combination of eqs. 1 and 2). However, in real practice, the growth ridge is unlikely to be prepared in a cross section exactly parallel to a (111) plane. Instead, it is either viewed from the side of the crystal (view direction <110> for growth in [001] direction), in the cross section perpendicular to the growth direction (*horizontal*) or in a cross section parallel to the growth direction (*vertical*, in a {110} plane for growth in [001] direction). The three mentioned views are depicted in Fig. 3. The further discussion is limited to the [001] growth direction. Therefore, only projections of the outer surfaces of individual facets are observed.

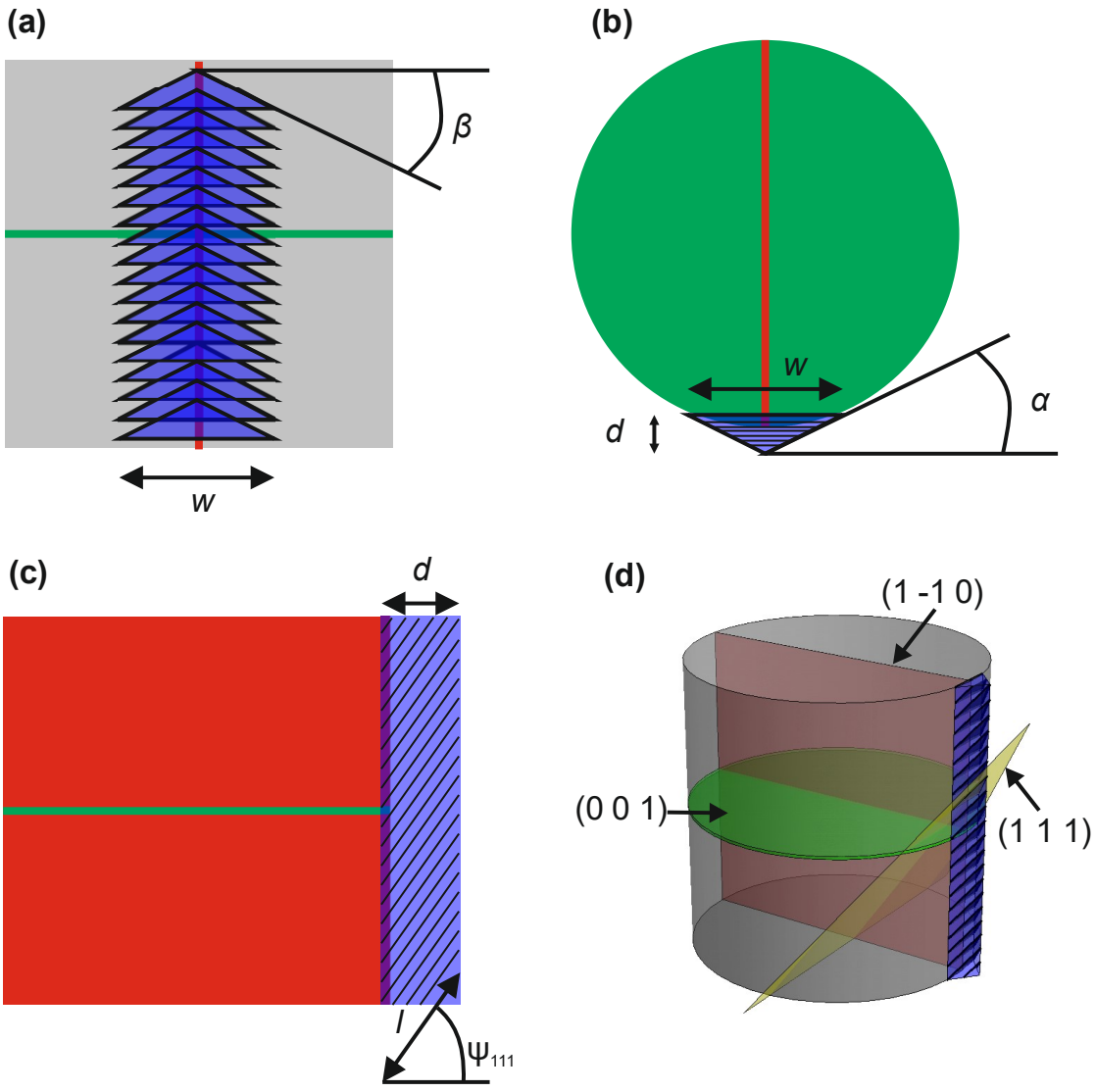

Fig. 3 Simplified geometry of the growth ridge and definition of the parameters width *w*, depth *d* and length l and the angles α and β. a) Frontal view, b) horizontal cross section c) vertical cross section and d) 3D view.

The observable angle α in the horizontal cross section is simply given by the ratio between the growth ridge width w and the growth ridge depth d:

$$\alpha = \tan^{-1}\left(\frac{2d}{w}\right) = \tan^{-1}\left(-\frac{\delta\phi_{\mathrm{m}}}{2}\right) \tag{4}$$

The angle β is geometrically connected to α by the fact that the border lines in both views are projections of straight lines located in the (111) plane. This yields

$$\beta = \cos^{-1}\left(\frac{\cos\alpha}{\sqrt{1+\sin^2\alpha}}\right). \quad (5)$$

Further, by resubstituting $d = \frac{\Delta T}{g_{\mathrm{facet}}}\sin\psi_{111}$ in eq. 3, one finds that the growth ridge width w can directly be calculated from the temperature gradient g_{facet} and vice versa:

$$w = \frac{4\sin\psi_{111}}{\chi\frac{g_{\mathrm{facet}}}{\Delta T} - \frac{2}{a}} \quad (6)$$

$$g_{\mathrm{facet}} = \frac{\Delta T}{\chi}\left(\frac{4\sin\psi_{111}}{w} + \frac{2}{a}\right) \quad (7)$$

This relation assuming $\chi = 22°$ (see below) is depicted in Fig. 4.

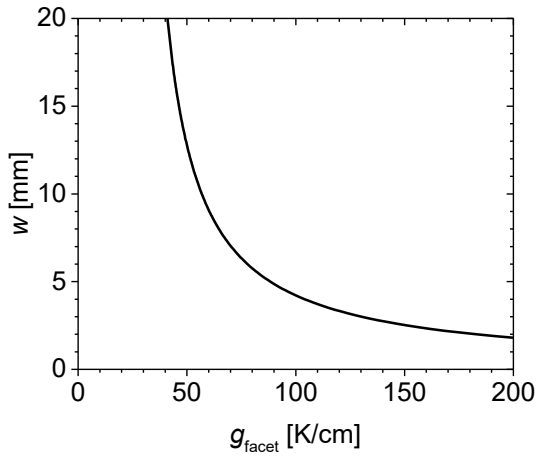

Fig. 4 Correlation between the temperature gradient g_{facet} in the direction parallel to the facet plane and the growth ridge width w.

3. Experimental determination of the growth ridge parameters

3.1 Characterization of the growth ridge topography

For the characterization of the growth ridge geometry, samples were chosen from various industrially grown, <100>-oriented, dislocation-free Si crystals with diameters of 125 mm

to 300 mm. All samples analyzed and discussed here were taken from the body parts of the crystals.

Samples were cut as segments of the cylindrical crystal with the growth ridge facing upwards. No preparation of the crystal's outer surface was carried out. The samples were scanned by an optical profilometer tool based on chromatic aberration with a depth resolution of 6 nm. The lateral step size was set to 20 µm.

A typical profile of the crystal surface exhibiting a growth ridge, extracted from a microscopic image of a horizontal cross section, is depicted in Fig. 5. In the vicinity of the growth ridge the deviation of the crystal shape from a perfect cylinder is rather complex: Besides the easily visible bump typically assessed as the growth ridge, which has a width of a few mm and mainly originates from the facet growth, the cylindrical shape is distorted in a much larger region. There is an additional protrusion beneath the bump with a width in the order of 20 mm, neighbored by a small depression (see Fig. 5b). These distortions might be attributed to the disturbance of the fluid dynamics / meniscus by the facetted growth. Actually, the solution of the Young-Laplace equation (see e.g. [11]) can yield a similar shape. Another possible explanation for this shape could be a slight variation of growth velocity in the different crystallographic directions.

Because of its complex nature, the term growth ridge is somewhat ambiguous and possibly used differently in previously published literature. In the present work, we concentrate on the external characterization of the edge facets. Thus, the definition of the growth ridge here is restricted to the part directly resulting from facet growth (it is marked by a green square in Fig. 5).

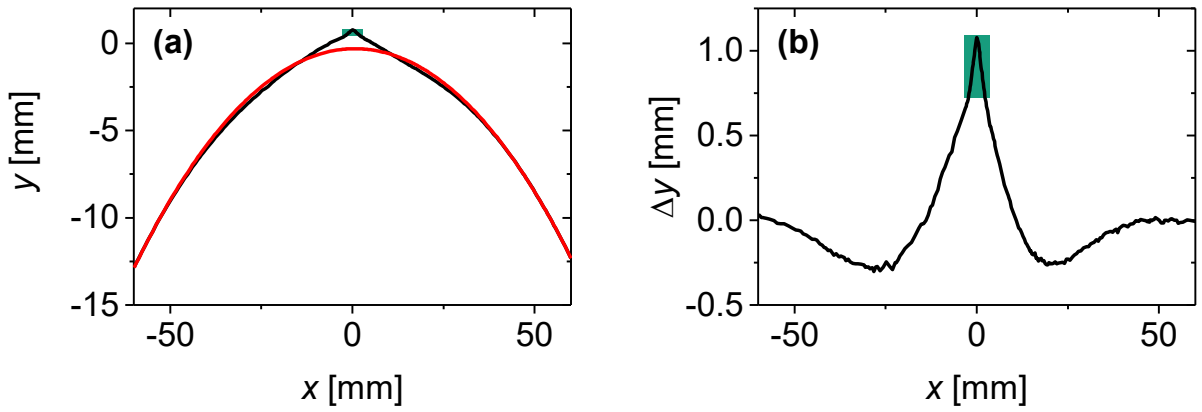

Fig. 5 Actual shape of the cross section of a 300mm Si wafer (black line) and perfect circle (red line) corresponding to the actual diameter of the wafer (305 mm). (b) Difference between the lines in (a). The green square marks the region of the growth ridge.

For characterizing the geometry of the growth ridge, we use the complete mapping of the surface profile after image processing, i.e. derivation of the image in *x* and *y* direction. The result of this procedure is shown in Fig. 6a. In analogy to the illustration in Fig. 3, the facets can be identified as straight lines which are not totally perpendicular to the pulling direction. According to the deliberations above, we define the growth ridge width w as the width of the region originating from facetted growth, i.e. the region where the slanted lines are visible. Using the corresponding topology profiles perpendicular to the growth direction, the height difference between the highest point and the baseline of w can be measured. This height difference is defined here as the growth ridge depth d. Furthermore, the angle β as described in Fig. 3a, can easily be extracted from such an image.

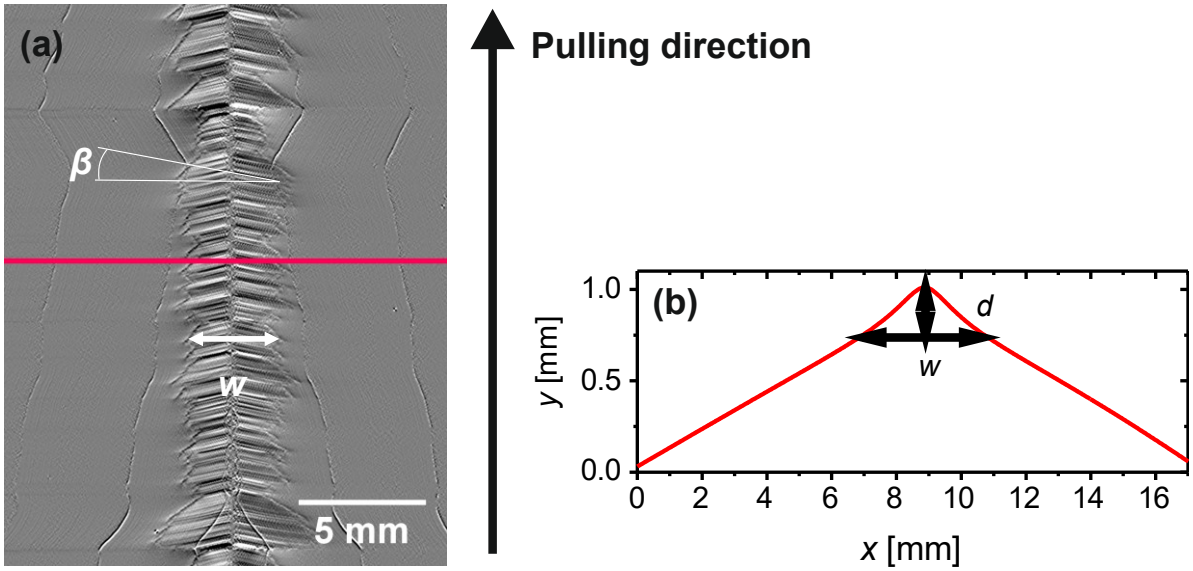

Fig. 6 (a) Top view of growth ridge topography after image processing. (b) Profile of the crystal surface at the position indicated by the red line in (a).

3.2 Characterization of the growth ridge cross section

In order to verify the results of the topography measurements, the growth ridges were also characterized on cross-sectional cuts by optical microscopy. To determine the size of the internal edge facets, samples were cut perpendicular to the pulling direction along the (001) plane (horizontal cross section). The samples were polished and etched in a Secco solution [14] to visualize the growth striations. For analysis, microscope images of the etched samples were taken.

Fig. 7 is an exemplary microscope image of the cross-section of a growth ridge along the (001) plane perpendicular to the pulling axis. The inner edge facets can be clearly identified as parallel lines (cf. Fig. 3b). For this method, the growth ridge width *w* is set as the length of the innermost straight striation ascribed to a facet. The growth ridge depth *d* then again is the distance between the innermost facet and the outermost point as indicated by the arrows in Fig. 7.

It is noteworthy that such a cross section immediately reveals that even the innermost facet extends to the crystal surface. This means that there is no facetted growth which remains invisible from the outside which encourages the approach to detect the facet parameters using the externally visible growth ridge as described above.

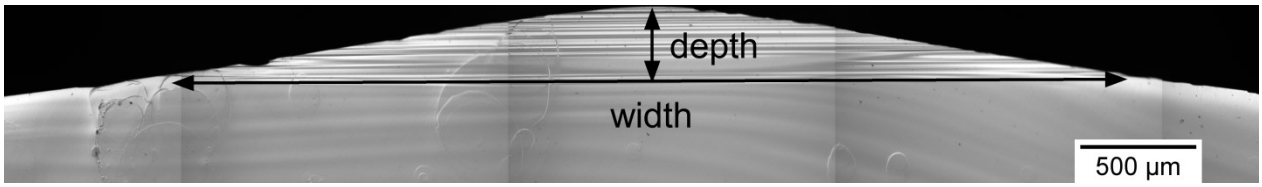

Fig. 7 Microscope image of the horizontal cross-section of a growth ridge after polishing and etching.

4. Results and Discussion

4.1. Validation of the experimental approach

In order to access the parameters required to describe the facet length and thereby the thermal field at the crystal surface, we evaluated the growth ridge width w and depth d for completely different crystals by either one of the two methods described above. In Fig. 8, these two values are plotted against each other. It is obvious that the data obtained by both methods agree very well with each other, verifying that both definitions for the growth ridge are equivalent.

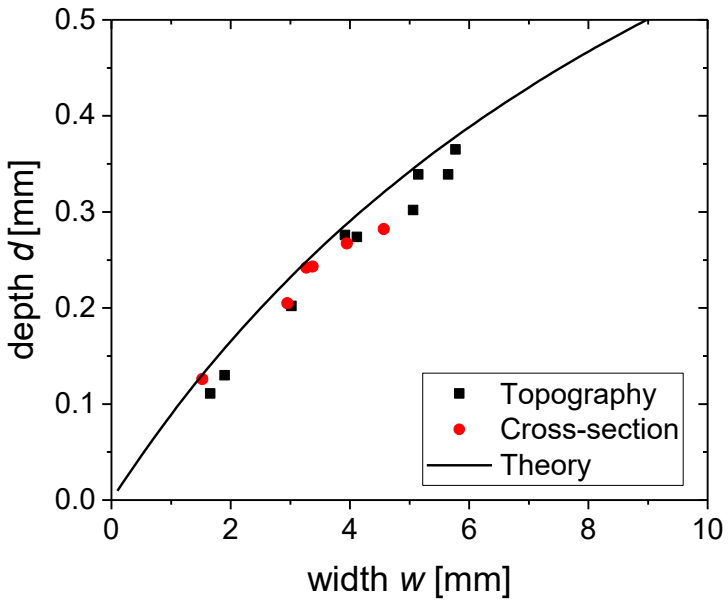

Fig. 8 Growth ridge width w and depth d from topography measurements and microscopic analysis of horizontal cross sections.

Furthermore, the experimentally obtained values agree remarkably well with the theoretically expected relation given in eq. 3. The only parameter to be adjusted was the angle χ, which was only estimated before by Voronkov ($\chi = 20°$ [9], $\chi = 25°$ [10]). The plot in Fig. 8 was obtained for $\chi = 22°$ which is used for all other calculations presented here. A slightly lower value for χ would yield an even better fit. However, it appears reasonable that the measured depth d slightly underestimates the physically relevant parameter because the "spire" of the growth ridge may easily be remelted or mechanically eroded, causing the outermost part of the growth ridge to be missing at the time of the measurement. Thus, we assume the growth ridge width w to be the more reliable parameter.

This result underlines both, the integrity of our measurement approach and the validity of Voronkov's model [10]. It also suggests that replacing the axial temperature gradient by the one in direction of the facet plane is reasonable. In his original publication [10],

Voronkov assumed the second term in eq. 1 to be negligibly small which would yield a linear dependence between w and d with a slope of the exact curve in the region of small w. From our data it is obvious that some industrially relevant crystal growth processes use temperature gradients small enough for this second term to be relevant. In these cases, the linear dependence is not a good approximation.

For a further test of our non-destructive characterization approach, we also investigated the angle β for different crystals. For that purpose, this angle was measured at various positions along the growth ridge, based on images similar to Fig. 6. The width w was similarly recorded along the growth ridge. For each crystal, mean values were calculated for both parameters and plotted against each other in Fig. 9. The given error bars are the standard deviations and include both errors due to the measurement as well as actual fluctuations of the parameters. Additionally, the theoretical prediction, which is obtained by combining eqs. 3, 4 and 5, is also plotted in that figure.

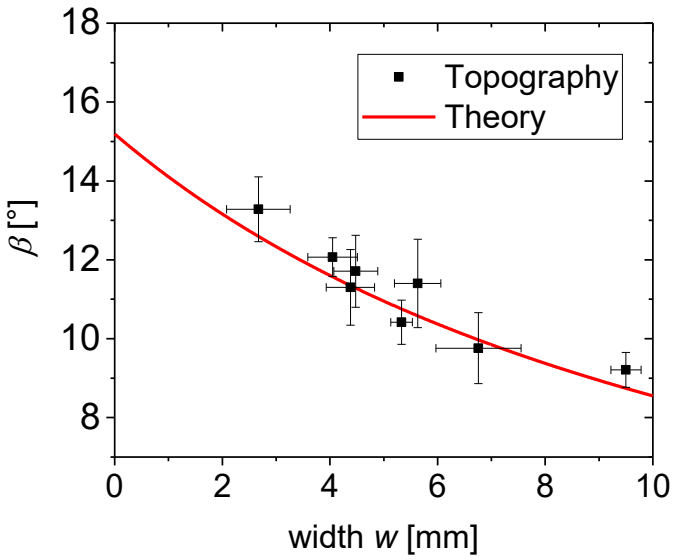

Fig. 9 Experimentally determined angle β plotted against the growth ridge width w for several different crystals together with the theoretical prediction.

Once again, the comparison between experimentally determined parameters and the theoretic prediction is remarkable. Thus, also the angle β could be used for analysis of the facet growth. However, we experienced that the determination of β is less accurate than that of the growth ridge width w. It is also noteworthy that the assumption of a negligible contribution of the finite temperature gradient in eq. 1 would yield a constant value of $\beta \approx 15°$ which is in obvious contradiction to our experimental findings.

4.2. Exemplary application

In Fig. 10, the growth ridge width w determined by the profilometer measurements along the growth direction, is shown for two crystals grown with different growth processes. The comparison illustrates that the geometry of the growth ridges can differ strongly for different processes: crystal 1 exhibits a growth ridge with a larger and almost constant width w, whereas the growth ridge of crystal 2 is smaller and fluctuates strongly.

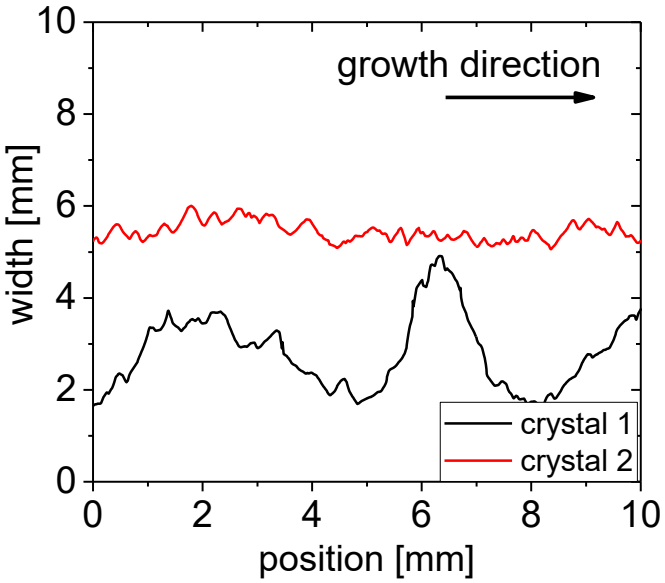

Fig. 10 Growth ridge width w for two crystals 1 and 2 along the growth direction.

As shown in the theory section, these fluctuations must be related to fluctuations of the thermal field. Qualitatively, this can already be assessed from the plot of the growth ridge width: Crystal 1 obviously was grown with an in general larger temperature gradient g_{facet} which also fluctuates much stronger. However, eq. 7 also allows quantifying these differences.

Fig. 11 shows the temperature gradients g_{facet} for both crystals along the growth direction, calculated from the measured growth ridge widths from Fig. 10. As can be seen, the growth process of crystal 2 features a temperature gradient of $g_{\mathrm{facet}} = (83.3 \pm 2.1)\mathrm{K/cm}$, which is lower, but much more stable than that of crystal 1 at $g_{\mathrm{facet}} = (145.1 \pm 33.6)\mathrm{K/cm}$ (errors are single standard deviations), oscillating between roughly 90 K/cm and 220 K/cm. Such an analysis enables the process surveillance and optimization regarding both

the absolute value of the temperature gradient at the crystal edge as well as on temperature fluctuations.

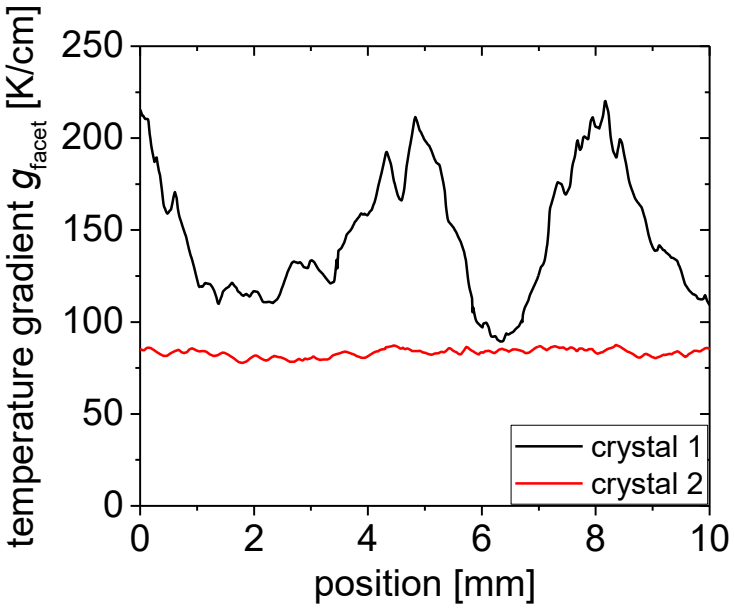

Fig. 11 Weighted temperature gradient g_{facet} along the pulling direction for two crystals grown by different growth processes.

5. Conclusion

We have developed a contactless, non-destructive experimental method to analyze the geometric parameters of crystal growth ridge and applied it to various Cz-grown Si crystals. The validity of this method has been verified by comparison to the data obtained from a microscopic analysis of etched samples and to theory. Our experimental results confirm the theory which allows calculating the temperature gradient at the growth ridge from any of the measured geometrical parameters, of which we have found the growth ridge width to be the most reliable and useful one. As a conclusion, not only the growth ridge can be used just to monitor dislocation-free growth in-situ, but also to get an easy

and direct access to the thermal conditions at the solid-liquid interface during the growth process which is highly valuable information for process surveillance and optimization.

6. Acknowledgements

Research and development published in this work were part of the projects *PowerOnSi* and *PowerBase*. PowerOnSi was funded partly by the European Regional Development Fund (ERDF) and by the Saxony State Ministry for Science and Art (SMWK). PowerBase has received funding from the Electronic Component Systems for European Leadership Joint Undertaking under grant agreement No 662133. This Joint Undertaking receives support from the European Union's Horizon 2020 research and innovation program and Austria, Belgium, Germany, Italy, Netherlands, Norway, Slovakia, Spain, United Kingdom.

6. References

[1] T. Duffar, Comprehensive review on grain and twin structures in bulk photovoltaic silicon, Recent Res. Devel. Crystal Growth (2009) 61–111.

[2] V.V. Voronkov, Theory of crystal surface formation in the pulling process, J. Crys. Growth 52 (1981) 311–318.

[3] V.V. Voronkov, Processes at the boundary of a crystallization front, Kristallografiya 19 (1974) 922–929.

[4] V.V. Voronkov, Face structure of crystals grown from a melt, Izvestiya Akademii Nauk SSSR. Seriya Fizicheskaya 47 (1983) 210–218.

[5] P. Rudolph, M. Czupalla, B. Lux, F. Kirscht, C. Frank-Rotsch, W. Miller, M. Albrecht, The use of heater-magnet module for Czochralski growth of PV silicon crystals with quadratic cross section, J. Crys. Growth 318 (2011) 249–254.

[6] T.F. Ciszek, Non-cylindrical growth habit of float zoned dislocation-free [111] silicon crystals, J. Crys. Growth 10 (1971) 263–268.

[7] K.B. Fritzler, E.M. Trukhanov, V.V. Kalinin, P.I. Smirnov, A.V. Kolesnikov, A.P. Vasilenko, Insitu Monitoring of Floating Zone-grown Si(111) crystal structurs using the behavior if ridgelike protrusions, Tech. Phys. Lett. 33 (2007) 521–523.

[8] O. Weinstein, S. Brandon, Dynamics of partially faceted melt/crystal interfaces II: multiple step–source calculations, J. Crys. Growth 270 (2004) 232–249.

[9] V.V. Voronkov, Mass transfer at the surface of a crystal near to its boundary with the melt, and its influence on the shape of the growing crystal, Kristallografiya 23 (1978) 249–256.

[10] V.V. Voronkov, Effects of facets at the crystallization front on crystal shape, Izvestiya Akademii Nauk SSSR. Seriya Fizicheskaya 49 (1985) 2467–2472.

[11] G. Barinovs, A. Sabanskis, A. Muiznieks, Numerical study of silicon crystal ridge growth, J. Crys. Growth 401 (2014) 137–140.

[12] G. Müller, J. Friedrich, Optimization and Modeling of Photovoltaic Silicon Crystallization Processes, in: AIP, 2010, pp. 255–281.

[13] T. Duffar, Crystal growth processes based on capillarity: Czochralski, floating zone, shaping and crucible techniques, Wiley, Chichester, West Sussex, Hoboken, N.J, 2010.

[14] F.S.d. Aragona, Dislocation etch for (100) planes in silicon, J. Electrochem. Soc.: Solid-State Science and Technology 119 (1972) 948–951.